TESTING OF FULL-SIZE REINFORCED CONCRETE BEAMS STRENGTHENED WITH FRP COMPOSITES: EXPERIMENTAL RESULTS AND DESIGN METHODS VERIFICATION

Final Report

SPR 387

Oregon Department of Transportation

TESTING OF FULL-SIZE REINFORCED CONCRETE BEAMS STRENGTHENED WITH FRP COMPOSITES: EXPERIMENTAL RESULTS AND DESIGN METHODS VERIFICATION

Final Report

SPR 387

by

Damian I. Kachlakev, PhD and David D. McCurry, Jr.
Oregon State University
Department of Civil, Construction and Environmental Engineering
202 Apperson Hall
Corvallis, Oregon 97331

for

Oregon Department of Transportation
Research Group
200 Hawthorne SE, Suite B-240
Salem, OR 97301-5192

and

Federal Highway Administration
400 Seventh Street SW
Washington, DC 20590

June 2000

1. Report No.	2. Government Accession No.	3. Recipient's Catalog No.
FHWA-OR-RD-00-19		

4. Title and Subtitle	5. Report Date
Testing of Full-Size Reinforced Concrete Beams Strengthened with FRP Composites: Experimental Results and Design Methods Verification	June 2000
	6. Performing Organization Code

7. Author(s)	8. Performing Organization Report No.
Damian I. Kachlakev, PhD and David D. McCurry, Jr. Oregon State University Department of Civil, Construction and Environmental Engineering 202 Apperson Hall Corvallis, Oregon 97331	

9. Performing Organization Name and Address	10. Work Unit No. (TRAIS)
Oregon Department of Transportation Research Group 200 Hawthorne SE, Suite B-240 Salem, Oregon 97301-5192	11. Contract or Grant No. SPR 387.11

12. Sponsoring Agency Name and Address		13. Type of Report and Period Covered
Oregon Department of Transportation Research Group 200 Hawthorne SE, Suite B-240 Salem, Oregon 97301-5192	and Federal Highway Administration 400 Seventh Street SW Washington, D.C. 20590	Final Report
		14. Sponsoring Agency Code

15. Supplementary Notes

16. Abstract

In 1997, a load rating of an historic reinforced concrete bridge in Oregon, Horsetail Creek Bridge, indicated substandard shear and moment capacities of the beams. As a result, the Bridge was strengthened with fiber reinforced polymer composites as a means of increasing load-carrying capacity while maintaining the historic appearance. Because composites were a relatively new construction material in infrastructure projects, subsequent tests were conducted to verify the design used on the Bridge. Four full-size beams were constructed to match the dimensions and strength capacity of the Bridge crossbeams as closely as possible. One of these beams was used as the control, while the other three beams were strengthened with various composite configurations including the same configuration used on the Bridge crossbeams. The beams were loaded in third point bending to determine their capacity. The beam strengthened with the same composite design used on the Bridge could not be broken with loading equipment used. Based on the maximum loads applied, the Bridge beams have at least a 50% increase in shear and a 99% increase in moment capacity over the unstrengthened condition. Design calculations show the Bridge beams now exceed the required shear and moment capacities.

17. Key Words	18. Distribution Statement
composite, fiber reinforced polymer, FRP, reinforced concrete, strengthening, bridge, design	Copies available from NTIS

19. Security Classification (of this report)	20. Security Classification (of this page)	21. No. of Pages	22. Price
unclassified	unclassified	36 + Appendices	

SI* (MODERN METRIC) CONVERSION FACTORS

APPROXIMATE CONVERSIONS TO SI UNITS

Symbol	When You Know	Multiply By	To Find	Symbol
		LENGTH		
In	Inches	25.4	millimeters	mm
Ft	Feet	0.305	meters	m
yd	Yards	0.914	meters	m
mi	Miles	1.61	kilometers	km
		AREA		
in^2	square inches	645.2	millimeters squared	mm^2
ft^2	square feet	0.093	meters squared	m^2
yd^2	square yards	0.836	meters squared	m^2
ac	Acres	0.405	hectares	ha
mi^2	square miles	2.59	kilometers squared	km^2
		VOLUME		
fl oz	fluid ounces	29.57	milliliters	mL
gal	gallons	3.785	liters	L
ft^3	cubic feet	0.028	meters cubed	m^3
yd^3	cubic yards	0.765	meters cubed	m^3
NOTE: Volumes greater than 1000 L shall be shown in m^3.				
		MASS		
oz	ounces	28.35	grams	g
lb	pounds	0.454	kilograms	kg
T	short tons (2000 lb)	0.907	megagrams	Mg
		TEMPERATURE (exact)		
°F	Fahrenheit temperature	5(F-32)/9	Celsius temperature	°C

APPROXIMATE CONVERSIONS FROM SI UNITS

Symbol	When You Know	Multiply By	To Find	Symbol
		LENGTH		
mm	millimeters	0.039	inches	in
m	meters	3.28	feet	ft
m	meters	1.09	yards	yd
km	kilometers	0.621	miles	mi
		AREA		
mm^2	millimeters squared	0.0016	square inches	in^2
m^2	meters squared	10.764	square feet	ft^2
ha	hectares	2.47	acres	ac
km^2	kilometers squared	0.386	square miles	mi^2
		VOLUME		
mL	milliliters	0.034	fluid ounces	fl oz
L	liters	0.264	gallons	gal
m^3	meters cubed	35.315	cubic feet	ft^3
m^3	meters cubed	1.308	cubic yards	yd^3
		MASS		
g	grams	0.035	ounces	oz
kg	kilograms	2.205	pounds	lb
Mg	megagrams	1.102	short tons (2000 lb)	T
		TEMPERATURE (exact)		
°C	Celsius temperature	1.8 + 32	Fahrenheit	°F

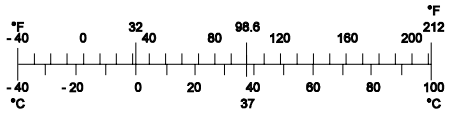

***** SI is the symbol for the International System of Measurement (4-7-94 jbp)

ACKNOWLEDGEMENTS

The authors wish to express special appreciation to Dr. Solomon Yim and Dr. Thomas Miller, professors at the Civil, Construction and Environmental Engineering Department at the Oregon State University for their valuable suggestions and help during this study. We would like to thank Mr. Andy Brickman and Professor John Peterson, both from the Civil, Construction and Environmental Engineering Department at the Oregon State University for their time and great help on conducting the experiments during this study.

The authors wish to extend special gratitude to Mr. Marty Laylor, Mr. Steven Soltesz, Project Managers, and Dr. Barnie Jones, Research Manager at the Research Unit of the Oregon Department of Transportation, Salem, Oregon for their valuable suggestions and many contributions to this project.

The authors would like to thank Mr. Ed Fyfe from Fyfe Corporation, LLC for donation of the FRP composites used in this project. Special appreciation goes to Mr. John Seim, Blue Road Research, Oregon for providing the necessary equipment and conducting the fiber optics measurements during the experimental part of this study. In addition, we would like to thank Contech Services, Specialty Restoration Contractors from Vancouver, Washington for their help of preparing the specimens for FRP application.

In addition, we would like to thank the following graduate students from the Civil, Construction and Environmental Engineering Department at the Oregon State University, without whose help this study would have being an enormous challenge: Bryan Green, William Barnes, Tae-Woo Kim, Tanarat Potisuk, Dharadon Seamanontaprinya, and Kasidit Chansawat.

Finally, we would like to extend our appreciation to Professor Chris A. Bell, Associate Dean of the College of Engineering at the Oregon State University for his support and interest in our work.

DISCLAIMER

TESTING OF FULL-SIZE REINFORCED CONCRETE BEAMS STRENGTHENED WITH FRP COMPOSITES: EXPERIMENTAL RESULTS AND DESIGN METHODS VERIFICATION

TABLE OF CONTENTS

LIST OF TABLES

LIST OF FIGURES

1.0 INTRODUCTION

1.1 SIGNIFICANCE OF THE RESEARCH

Nearly 40 percent of the bridges in the United States and Canada are structurally deficient (Cooper 1991, FHWA 1993, Rizkalla & Labossiere 1999, FHWA 2000). Structural elements composed of concrete and reinforcing steel are frequently rated as inadequate due to load conditions beyond the capacity of the original designs. In addition, degradation such as corrosion and fatigue has reduced the capacity of many structures. External post-tensioning, addition of steel plating and total replacement have been the traditional methods used to meet the need for increased load capacity.

In recent years, fiber reinforced polymers (FRP) have been used to increase the capacity of reinforced concrete structural elements. Fiber reinforced polymers are typically comprised of high strength fibers (e.g. aramid, carbon, glass) impregnated with an epoxy, polyester, or vinyl ester resin (often termed the matrix). As this study showed, the addition of these materials can dramatically change the load capacity as well as the failure mechanism of reinforced concrete beams.

Experimental studies have been conducted using FRP reinforcing on both beams and columns. Field application of FRP is common, but a complete understanding of the behavior of reinforced concrete (RC) beams retrofitted with FRP is still lacking. This study investigated the bending behavior by way of strain and deflection of full-size beams in more detail than any previously known study.

1.2 HORSETAIL CREEK BRIDGE

The Oregon Department of Transportation (ODOT) is currently undertaking an ongoing effort to load rate all state and local agency owned bridges. Bridge evaluation is required by the Federal Highway Administration, which partially funds state and local bridge construction projects.

The load rating process involves careful inspection and rating of each structural element in a bridge according to prescribed methods. The lowest rated bridge member determines the rating for the bridge. If the bridge is determined deficient, the bridge owner is required to either retrofit, replace, or post the bridge.

Horsetail Creek Bridge, shown in Figures 1.1 and 1.2, is located east of Portland, Oregon along the Historic Columbia River Highway. It was designed and constructed by K.S. Billner and opened to traffic in 1914. The structure is an 18.3 m (60 ft) long simple 3-span reinforced concrete slab-beam-column structure. The length and width of each span is 6.1 m (20 ft). A photograph of the original bridge is shown in Appendix A.

The Horsetail Creek Bridge beams were constructed without shear reinforcement (required by current standards and knowledge of RC beam behavior). Shear reinforcement inhibits the development of diagonal tension cracks (shear cracks). Once formed, these cracks can propagate quickly and result in a sudden failure before full flexural capacity of the beam is achieved. For this reason, a minimal amount of reinforcement (usually steel stirrups) must be provided (ACI 318-99). Adequate spacing in high shear regions enables the reinforcement to effectively mitigate diagonal tension cracking.

Load rating of Horsetail Creek Bridge identified flexural and shear Rating Factors of RF = 0.5 and RF = 0.06, respectively (CH2M HILL, 1997). An RF value less than 1 indicates a deficient structure. The exceptionally low rating factor for shear was due to the lack of shear stirrups, which required the load-rating engineer to use only the concrete section to resist the induced shear forces. The details of the load rating, including selected calculations, are presented in Appendix B. It should be noted that visual inspection revealed minimal signs of distress or environmental degradation. Only a few locations of exposed steel under the bridge railing and curb were visible.

Figure 1.1: Horsetail Creek Bridge (1998, prior to retrofit)

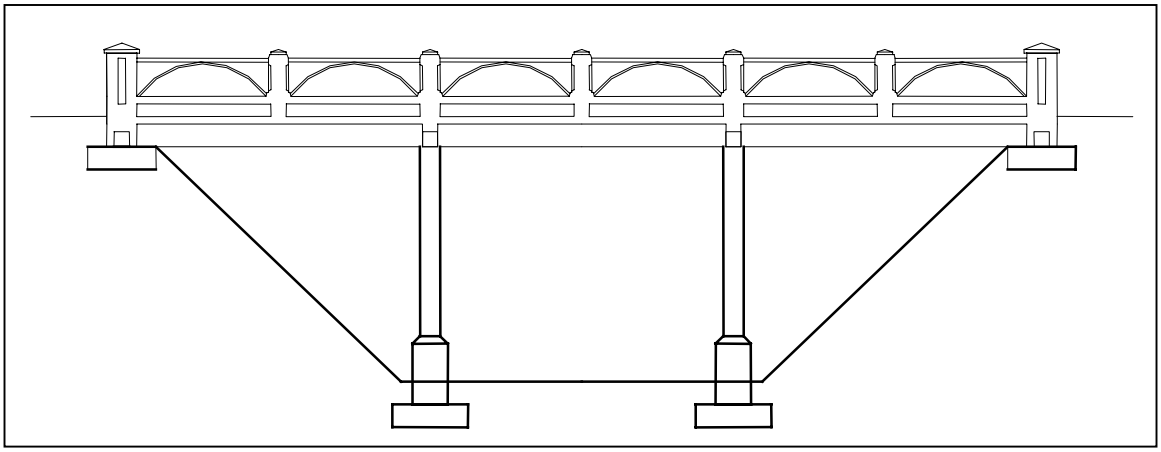

Figure 1.2: Elevation of Horsetail Creek Bridge (No. 04543)

As a consequence of the load rating, the Bridge was strengthened to an HS20 truck loading capacity using glass and carbon FRP. Of the strengthening options considered, FRP provided the required strength improvement and maintained the historic appearance of the Bridge.

1.3 PURPOSE OF THE STUDY

This study examined the increased load capacity as the result of FRP added to inadequate RC beams. In addition, this study investigated the bending behavior of reinforced concrete beams retrofitted with FRP by examining deflection and strain as a function of load. Laboratory testing was conducted on full-size beams that closely represented the Horsetail Creek Bridge beams in order to accomplish the following:

- To verify that the retrofit scheme used to strengthen the Horsetail Creek Bridge was sufficient for the traffic loads; and

- To provide experimental data to validate finite element models being developed in another research project.

A secondary objective was to evaluate the effectiveness of a fiber optic strain sensing system for monitoring strain in FRP strengthened beams. Under a separate study, fiber optic strain sensors were installed on Horsetail Creek Bridge to monitor static, dynamic and long-term load response. This project was part of a continuing effort to use fiber optic sensors for structural health monitoring.

2.0 TEST SETUP

2.1 BEAM CONSTRUCTION AND PROPERTIES

Four full-scale beams with similar geometry and rebar placement as the Horsetail Creek Bridge crossbeams were constructed in the Oregon State University laboratories. Figure 2.1 shows the beam dimensions and the location of the rebar. There were three main flexural steel bars extending the full length and two bars that bent up to reinforce negative moment regions of the beam. Smaller diameter bars were positioned near the compression face of the beam.

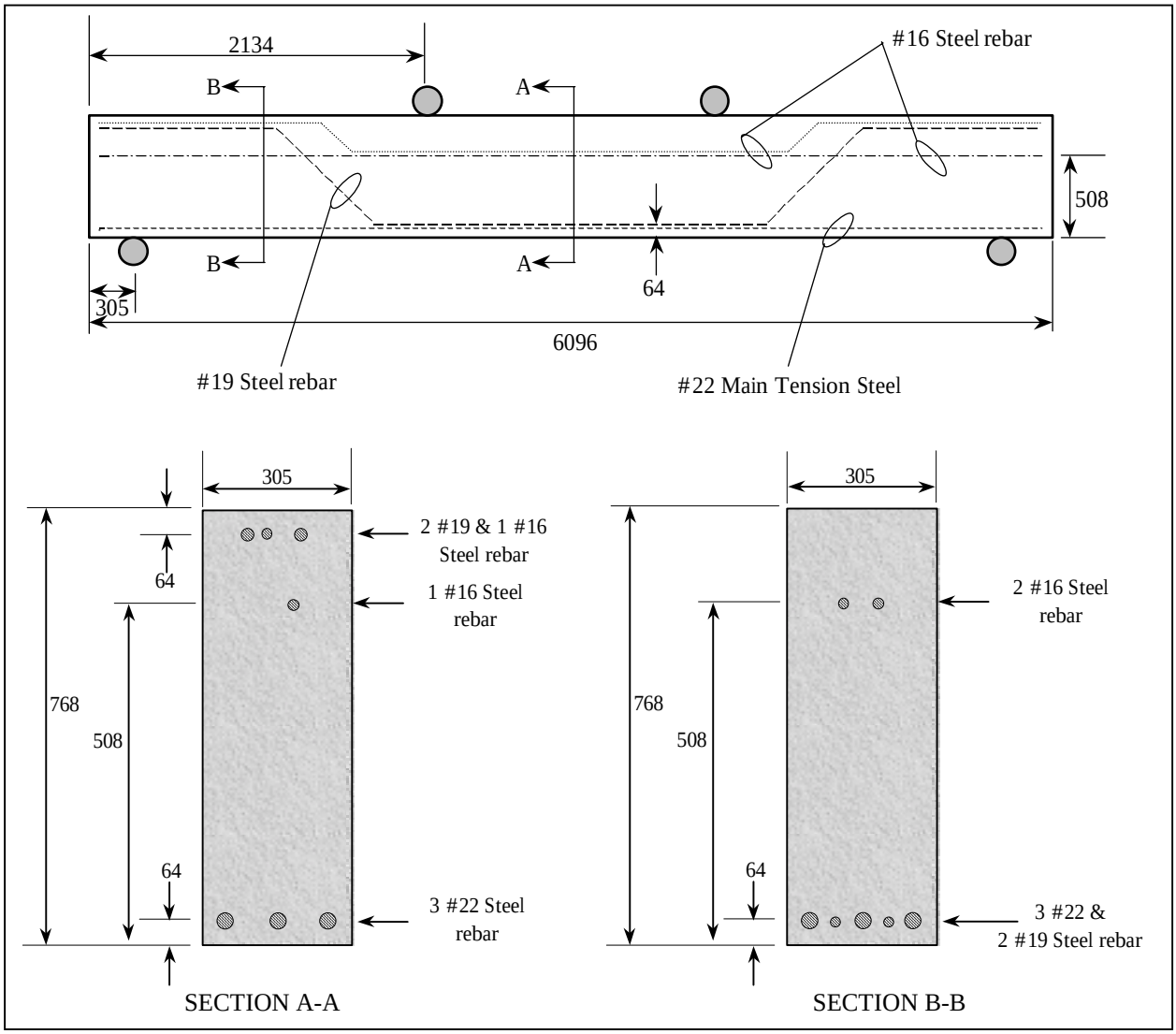

Figure 2.1: Position of steel reinforcement in all beams. Dimensions and rebar sizes are in mm.

The beams were designed to match the strength rather than the serviceability of the Horsetail Creek Bridge beams. For load rating purposes, AASHTO specifies the concrete strength of a bridge constructed before 1959 to be 2500 psi (17.2 MPa) and the steel yield stress to be 33,000 psi (228 MPa) (AASHTO, 1994). Concrete and steel are not readily available at these low strength levels. In an effort to construct beams with similar ultimate strength as the Horsetail Creek Bridge beams, reinforcement bars with smaller cross-sectional areas, Table 2.1, were used to account for the higher yield strength of today's steel. Design calculations for the beams are provided in Appendix B.

Table 2.1: Steel reinforcement details

Standard Bar Size	Metric Bar Size	Steel Area	Location of Reinforcement
#5	#16	0.31 in^2 (200 mm^2)	Straight and bent steel above elastic neutral axis. Derived from bridge deck reinforcement
#6	#19	0.44 in^2 (280 mm^2)	Bent reinforcement used for positive and negative moment reinforcement.
#7	#22	0.60 in^2 (390 mm^2)	Straight positive moment reinforcement bars present in all bridge beams.

The four beams were cast and cured separately under similar conditions. Type I ready-mix concrete with nominal 28-day strength of 3000 psi (20.7 MPa) and 6 in (152 mm) slump was used. The beams were cast in the same form to ensure the dimensions were as similar as possible. Each beam was cured in a moist condition until removed from the form 7-14 days after pouring. Ambient conditions during casting and curing did not vary significantly from beam to beam.

After curing, three of the four full-size beams were strengthened with FRP. A description of each beam is given in Table 2.2, and the FRP configurations are shown in Figure 2.2. The Control, Flexure-Only, Shear-Only, and Shear and Flexure beams will be referred to as the Control Beam, F-Only Beam, S-Only Beam, and S&F Beam in this report. Table 2.3 shows the material properties used for analysis, which are based on established design values.

Table 2.2: Experimental beam description[1]

Beam	Description
Control	Reinforced concrete beam with no shear stirrups and no FRP reinforcement
Flexure-only	Control beam with added flexural carbon FRP reinforcement
Shear-only	Control beam with added shear glass FRP reinforcement
Shear & Flexure	Control beam with added shear and flexural reinforcement

[1]See also Figure 2.2.

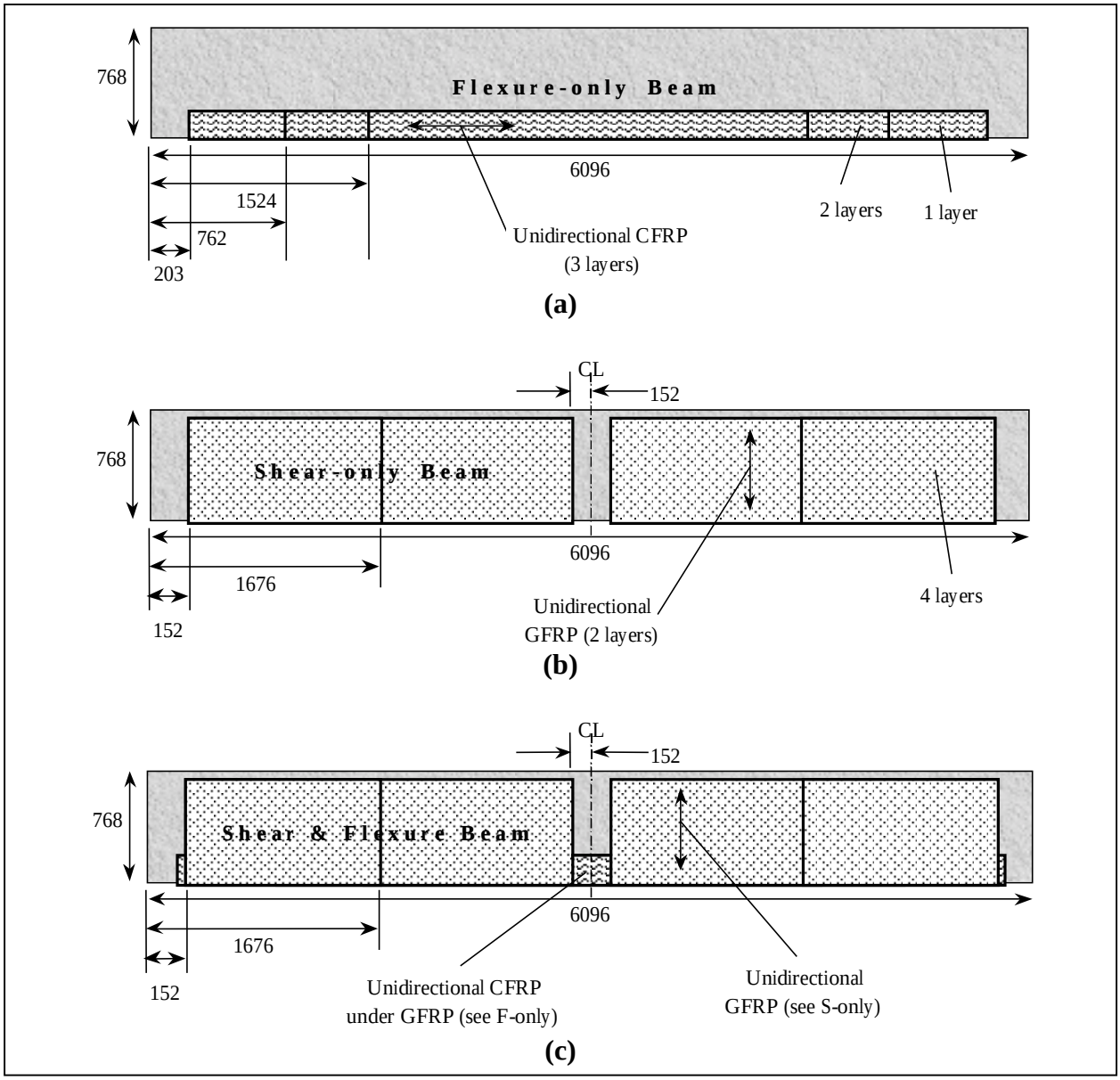

Figure 2.2: FRP-strengthened experimental beams. The flexural and shear FRP composites were wrapped continuously around the bottom of the beam. All dimensions in mm.

Table 2.3: Design material properties

Material	Limiting Stress	Limiting Strain	Limit State	Elastic Modulus
Concrete (Compression)	3000 psi (20.7 MPa)	0.003	Crushing	3120 ksi[1] (21.5 GPa)
Steel Reinforcement	60 ksi (414 MPa)	0.002	Yielding	29,000 (200 GPa)
Glass FRP	60 ksi (414 MPa)	0.02	Rupture	3000 ksi (20.7 GPa)
Carbon FRP	110 ksi (760 MPa)	0.012	Rupture	9000 ksi (62 GPa)

[1]Design elastic modulus from $E_c=57{,}000(f_c')^{1/2}$.

2.1.1 Concrete Modulus Determination

Efforts were made to accurately determine the actual elastic moduli of the beams so that a correct estimation of beam stiffness could be made. A correlation was made between pulse velocity and compressive elastic modulus (ASTM 1983, 1994). From this work, it was determined that each beam possessed a slightly different elastic modulus, as shown in Table 2.4. The elastic moduli calculated from cylinder strengths were too high in comparison to the elastic moduli determined from design 28-day strength and the pulse velocity measurements.

Table 2.4: Elastic modulus results from pulse velocity correlation[1]

Beam	Average Measured Pulse Velocity (km/s)	Elastic Modulus from Correlation
Control	3.72	2,810,000 psi (19.3 GPa)
Flexure-only	3.53	2,550,000 psi (17.6 GPa)
Shear-only	3.60	2,63,000 psi (18.2 GPa)
Shear & Flexure	3.48	2,480,000 psi (17.1 GPa)

[1] Correlation between ASTM C 469 and ASTM C 597 was conducted.

2.2 TESTING AND DATA COLLECTION

Details about data acquisition and the equipment used are found in Appendices C & D. A summary of the testing and data acquisition methods is presented below.

2.2.1 Beam Loading

All beams were tested in third-point bending as shown in Figure 2.3. No restraint was provided against rotation along any axis. Supports did not provide any fixity aside from friction due to normal forces. Thus, the beams could be analyzed as simply-supported beams. All beams spanned 18 ft (5.49 m) with a shear-span of 6 ft (1.83 m).

A 600 kip (2670 kN), internal-frame, hydraulic press with a load cell was used to load the beams. This machine was designed to compress test specimens by transferring all forces into its own frame. For beams that spanned beyond the frame of the machine (the situation for the beams in this project), the maximum applied force was limited to 160 kip (712 kN). This constraint was not known until after the project was initiated.

2.2.2 Data Collection

Deflection data were collected from three locations using direct current displacement transducers (DCDTs) as shown in Figure 2.3. A dial gauge was placed in the same longitudinal location as DCDT 2 to verify midspan deflection.

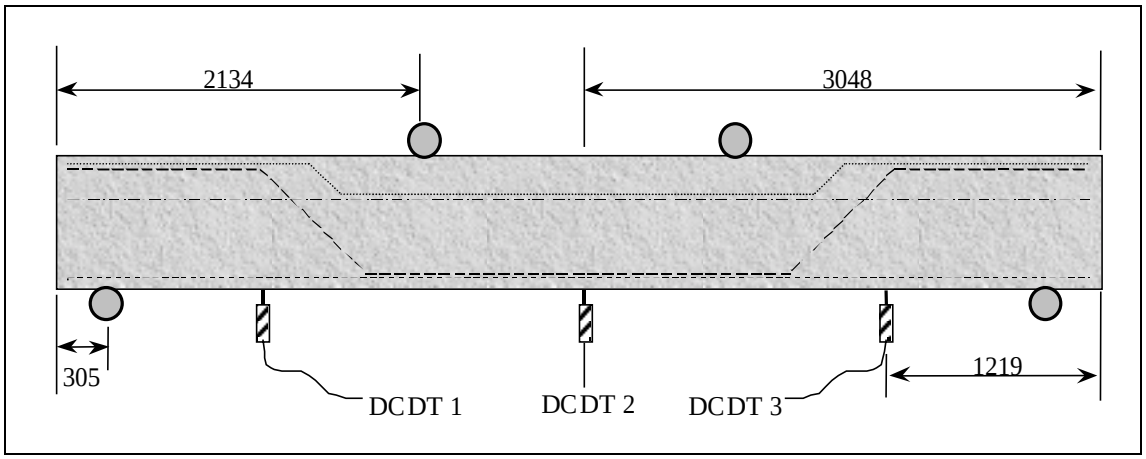

Figure 2.3: DCDT locations. Dimensions in mm.

Resistance strain gauges with a 2.36 in (60 mm) gauge length were placed at select sites throughout the beam. Strain data were collected at the midspan section and two sections in the shear zone as shown in Figure 2.4. Other important strains were collected as needed. Gauges were placed on the concrete surface, on the FRP surface, or inside the beam on the steel. Fiber optic gauges were installed only on the three FRP-reinforced beams in the positions shown in Figure 2.5. The fiber optic gauges were monitored by Blue Road Research[1] during the tests.

In order to ensure data collection systems were properly responding to applied loads, three cycles up to 15 kip (67 kN) were made. The load cycling helped to identify "noisy" and inadequate data collection channels in addition to providing more data for finite element models being developed under a separate project.

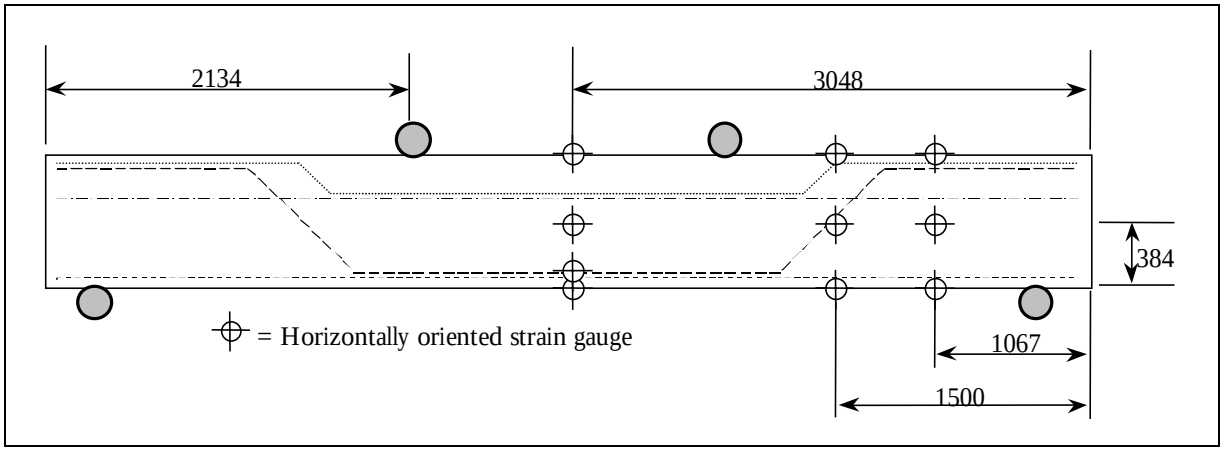

Figure 2.4: Typical locations of resistance strain gauges. Dimensions in mm.

[1] 2555 NE 205th Avenue, Fairview, Oregon 97024. See: www.bluerr.com

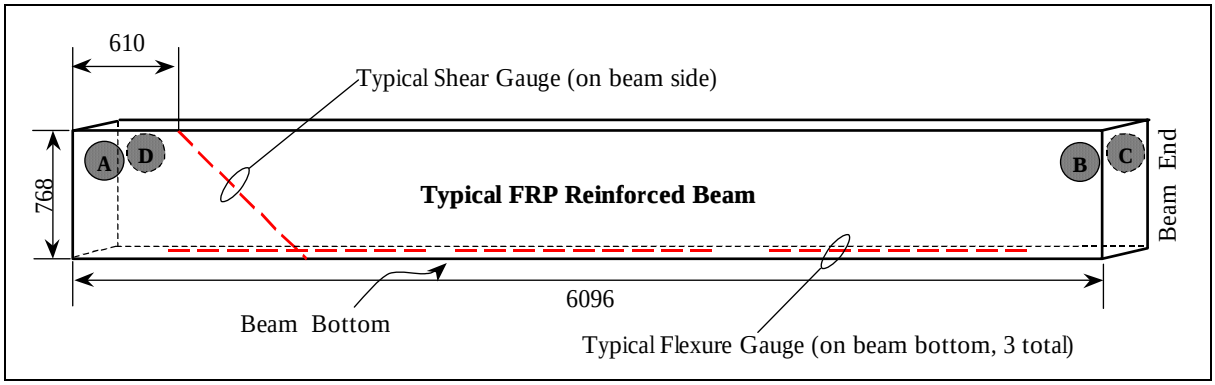

Figure 2.5: Locations of fiber optic strain gauges. Dimensions in mm.

Cracking was documented during the testing. Only the Control Beam and to a lesser degree, the F-Only Beam, provided a good map of the cracks because the S-Only and S&F Beams were wrapped with FRP laminates on the sides. Appendix C gives a complete description of visible cracking patterns. For this experimental study, crack widths were not measured.

3.0 EXPERIMENTAL RESULTS

3.1 SUMMARY OF LOAD AND DEFLECTION

The Control, F-Only and S-Only beams were loaded to failure. The failure modes are shown in Table 3.1. The S&F Beam was loaded to 160 kip (712 kN), the capacity of the testing equipment, and held for several minutes without failing. The S&F Beam was reloaded to 160 kip (712 kN) with the load points positioned 2 ft (51 mm) apart to increase the applied moment and again held at this load for several minutes. There was no indication of imminent failure.

Table 3.1: Beam failure modes

Beam	Failure Mode
Control	Diagonal tension crack (shear failure)
Flexure-only	Diagonal tension crack (shear failure)
Shear-only	Yielding of tension steel followed by crushing of compression concrete after extended deflections
Shear & Flexure	No failure observed. Believed to be yielding of tension steel followed by crushing of the concrete. FRP rupture might occur after significant deflections due to failure of the concrete

A summary of the capacity and deflection results is presented in Table 3.2. A load of 15 kip (67 kN) was selected for comparing deflection, and hence stiffness, before first significant cracking. First significant cracking is indicated by the sudden change in slope at approximately 20 kip. Stiffness after first significant cracking was calculated from the slope of the load-deflection curve after cracking.

Figures 3.1 to 3.4 show the load vs. deflection plots for the four beams. Midspan deflection for the S-Only Beam went beyond the range of the DCDT2. Consequently, part of the plot is shown as an extrapolated line. For all plots used in this study, the applied moment at the midspan in kip-ft is always three times the applied load in kip based on the relationship M=PL/3 where P is ½ the total applied load and L is the span length. The applied moment in kN-m is 0.914 times the load in kN. The applied shear is 1/2 the applied load.

Table 3.2: Summary of load and deflection

Item	Control	Flexure-Only	Shear-Only	Shear & Flexure
Midspan Deflection at 15 kip (67 kN)	0.0465 in (1.18 mm)	0.0480 in (1.22 mm)	0.0489 in (1.24 mm)	0.0435 in (1.10 mm)
Stiffness After First Significant Cracking[1]	115 kip/in (20.1 kN/mm)	139 kip/in (24.3 kN/m)	134 kip/in (23.5 kN/m)	150 kip/in (26.3 kN/m)
Midspan Deflection at Steel Yield[2]	Did Not Yield	Did Not Yield	0.896 in (23 mm)	Did Not Yield
Maximum Observed Deflection	0.963 in (24.5 mm)	1.193 in (30.3 mm)	1.390 in (35 mm)[3]	1.000 in (25 mm)
Midspan Deflection at Failure	0.963 in (24.5 mm)	1.193 in (30.3 mm)	2.00 in (51 mm)[3]	Did Not Fail[4]
Load at First Significant Cracking[1]	17.6 kip (78.3 kN)	21.7 kip (96.5 kN)	19.7 kip (87.6 kN)	21.6 kip (96.1 kN)
Load at Failure	107 kip (476 kN)	155 kip (689 kN)	155 kip (689 kN)	Did Not Fail[4]
Applied Moment at Yield[2]	Did Not Yield	Did Not Yield	360 kip-ft (488 kN-m)	Did Not Yield
Maximum Applied Moment[4]	321 kip-ft (435 kN-m)	465 kip-ft (630 kN-m)	465 kip-ft (630 kN-m)	480 kip-ft (651 kN-m)[5]
Maximum Applied Shear	53.5 kip (234 kN)	77.5 kip (345 kN)	77.5 kip (345 kN)	80.0 kip (356 kN)

[1]First significant cracking is indicated by the first slope change of the load-deflection plot.
[2]Primary tension reinforcement only yielded in the S-Only Beam.
[3]Extrapolated.
[4]S&F Beam was not loaded to failure due to equipment limitations.
[5]A second loading of the S&F Beam achieved a total applied moment of 640 kip-ft (868 kN-m).

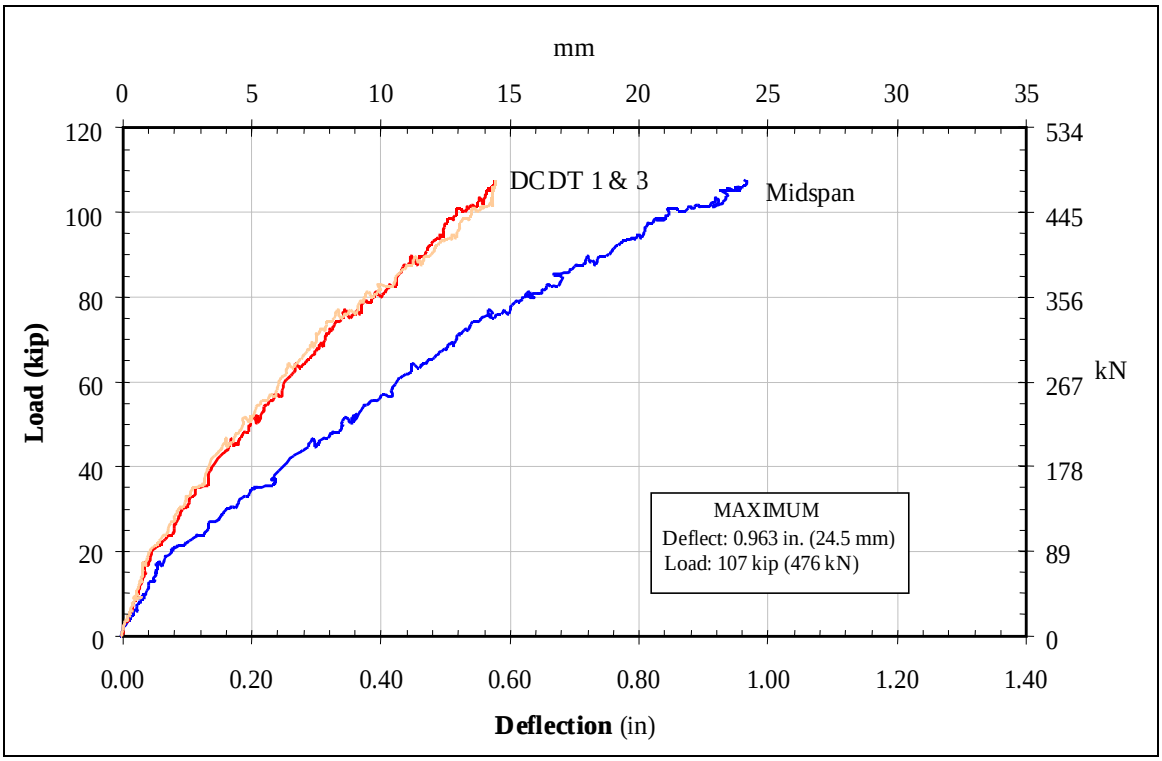

Figure 3.1: Load vs. deflection for the Control Beam

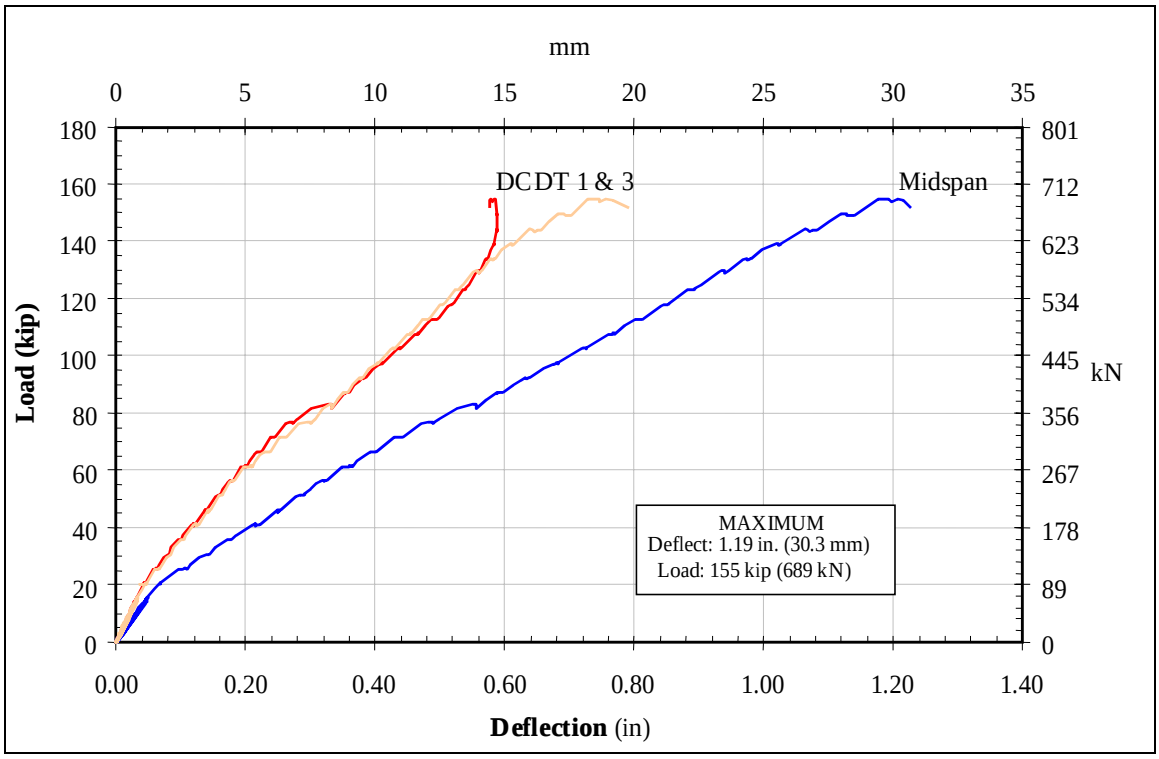

Figure 3.2: Load vs. deflection for the Flexure-Only Beam

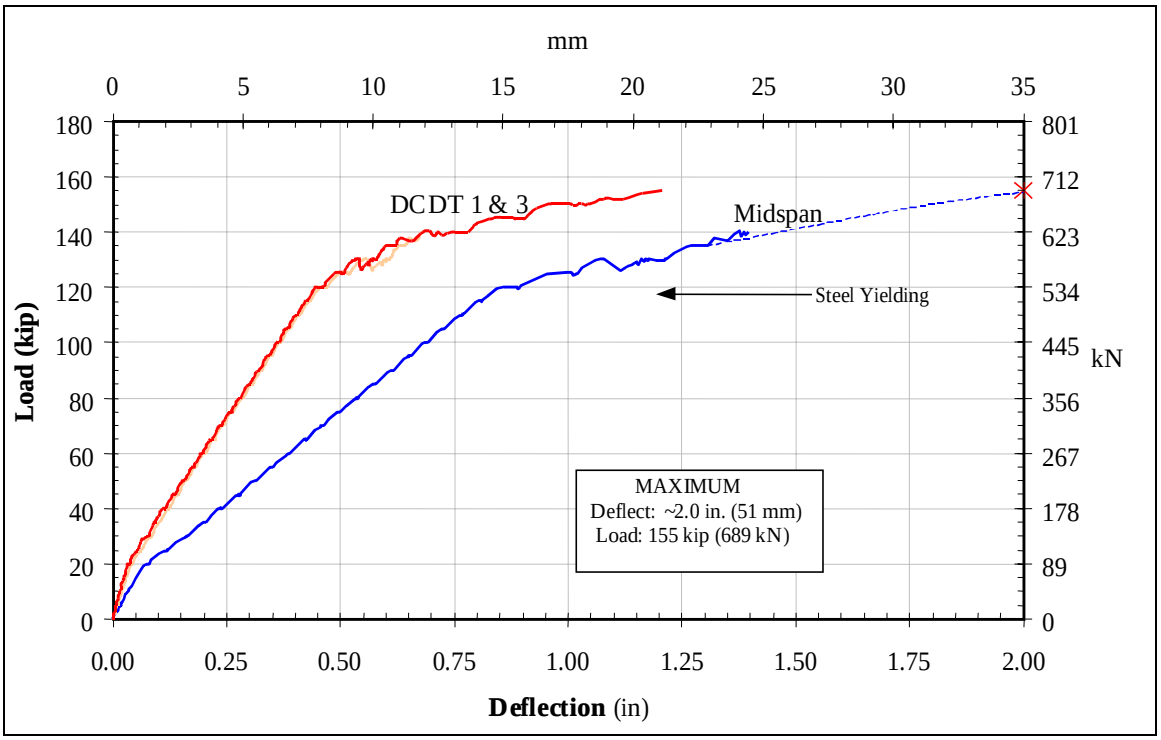

Figure 3.3: Load vs. deflection for the Shear-Only Beam

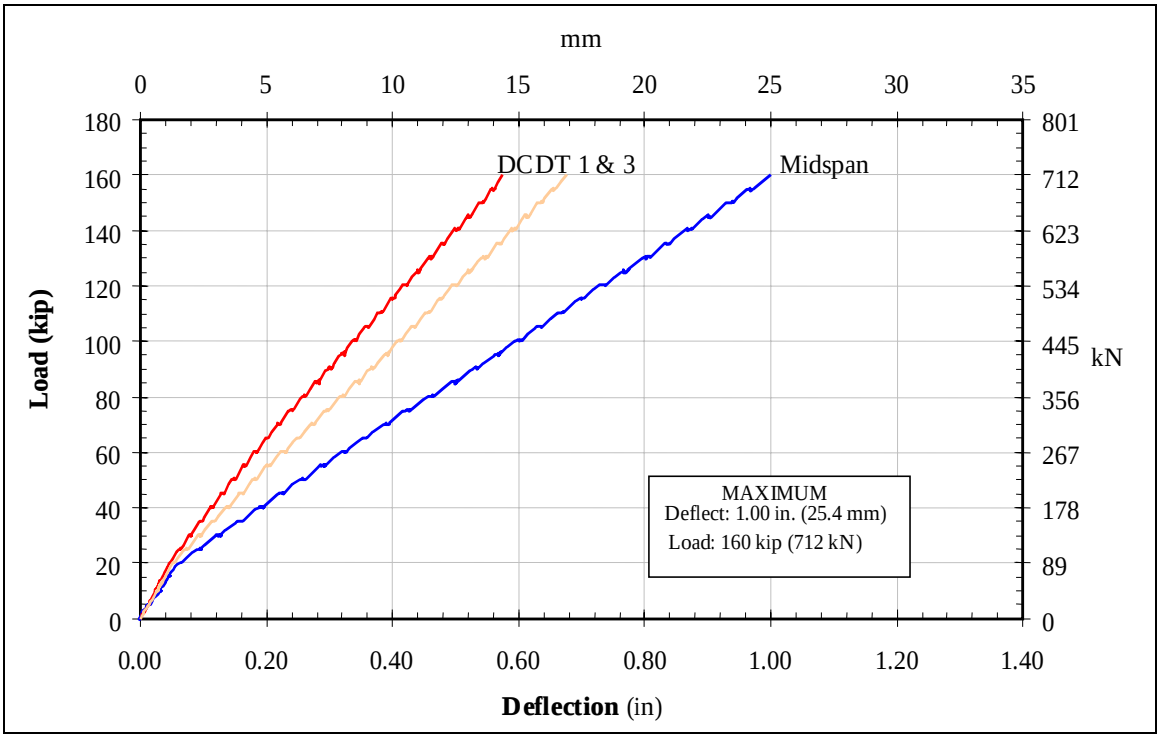

Figure 3.4: Load vs. deflection for the S&F Beam (beam did not fail)

3.2 STRAIN DATA

Appendix C presents the load vs. strain data. Figures 3.5 to 3.8 provide midspan strain as a function of load for the four beams. The steel yielding in the S-Only Beam is indicated in Figure 3.7. Figure 3.8 shows the strain in the tension steel reinforcement of the S&F Beam had just exceeded the design limit strain of 0.002. Consequently, the anticipated failure mode for the S&F Beam was flexural failure characterized by steel yielding followed by concrete crushing.

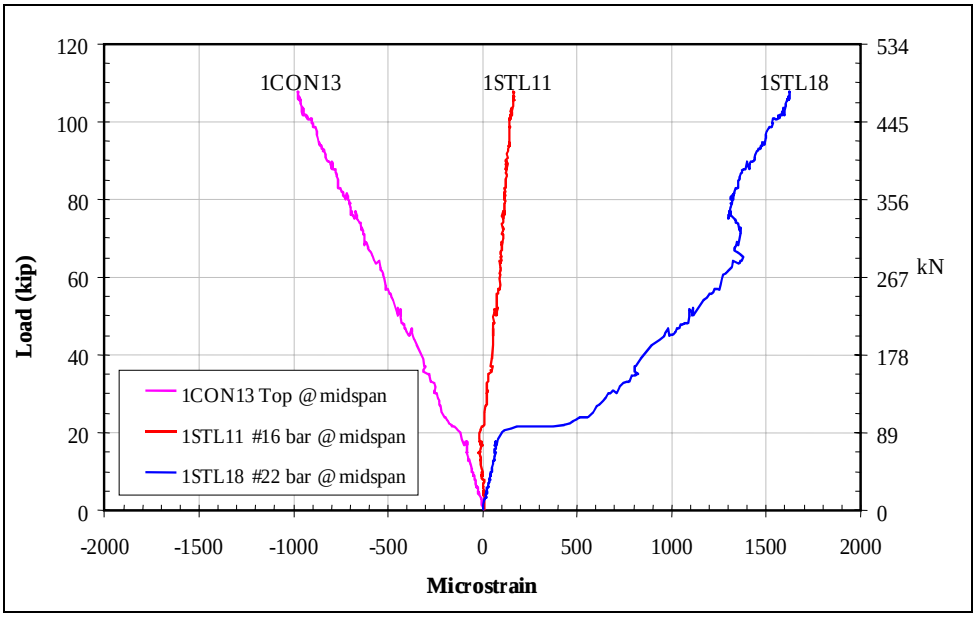

Figure 3.5: Control Beam load vs. strain at midspan

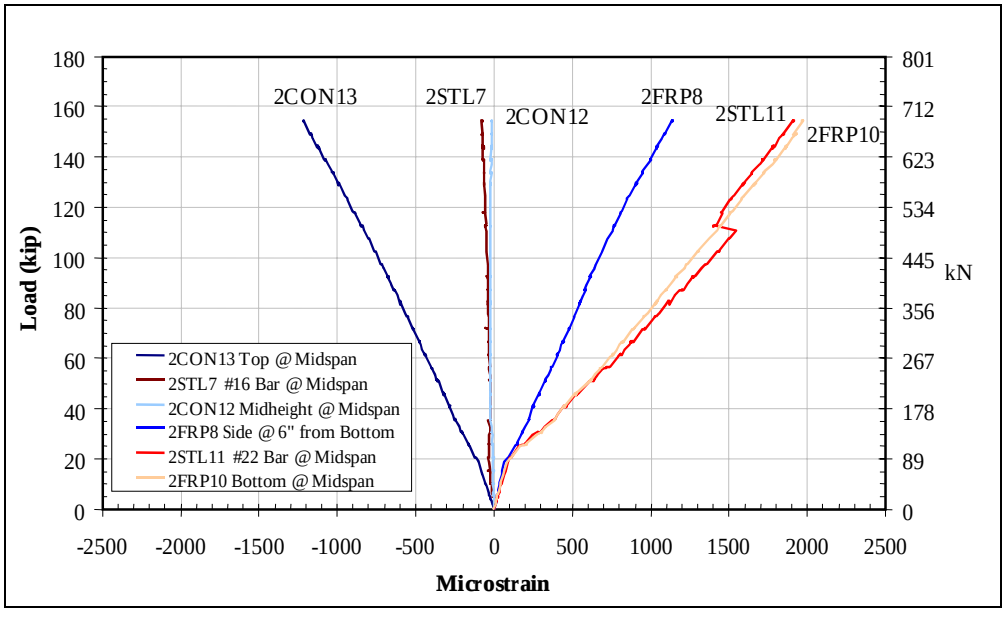

Figure 3.6: F-Only Beam load vs. strain at midspan

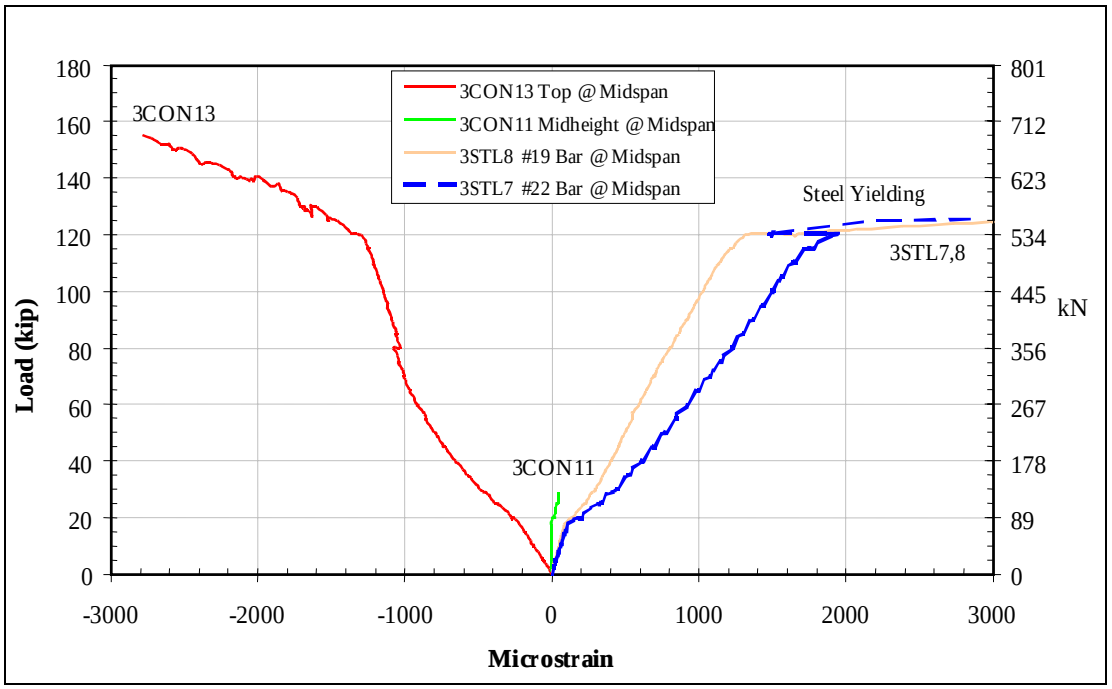

Figure 3.7: S-Only Beam load vs. strain at midspan

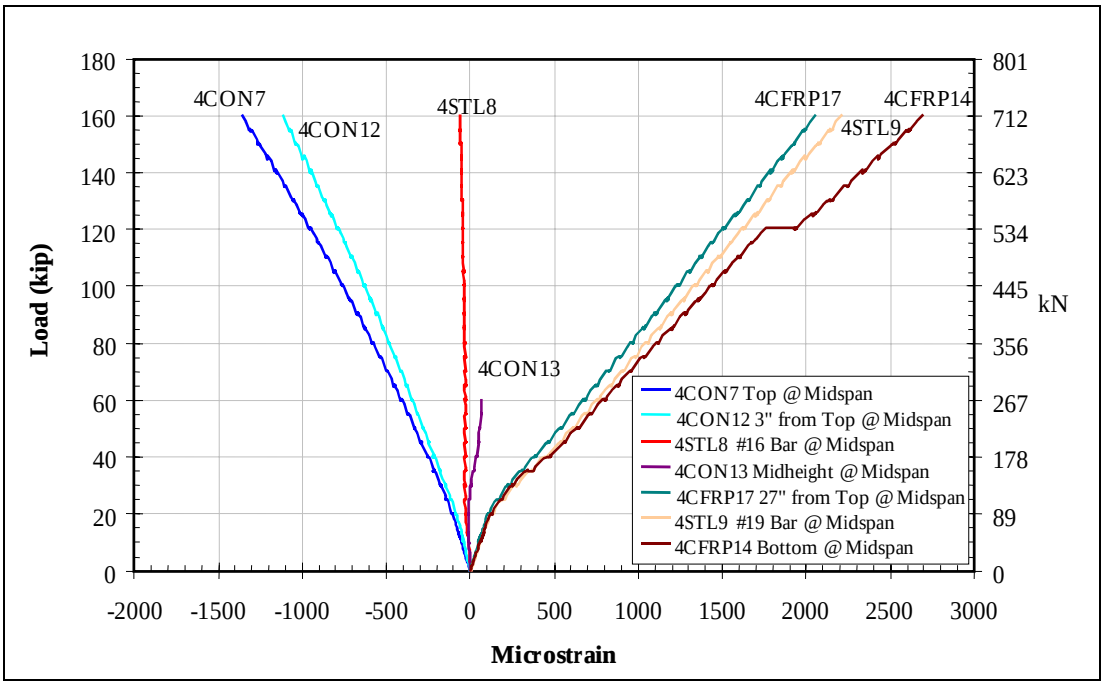

Figure 3.8: S&F Beam load vs. strain at midspan

4.0 INTERPRETATION AND DISCUSSION OF EXPERIMENTAL RESULTS

4.1 GAINS OVER THE CONTROL BEAM

Table 4.1 and Figure 4.1 compare the experimental results of the four beams. Important observations include the following:

- The F-Only and S-Only beams had the same increase in load, 45% greater than the Control Beam, but failed in different modes.
- The first load test of the S&F Beam revealed at least a 50% increase in load and moment capacity. The second load test showed that the S&F Beam had at least 99% greater moment capacity than the Control Beam.
- Post cracking stiffness increased up to 30% with the FRP strengthening.
- The addition of FRP in shear and flexure both independently and as a combined system allowed for greater deflections at failure.
- All reinforced beams cracked at higher loads than the unstrengthened Control Beam.

Post cracking stiffness was increased as a result of FRP application. The flexural CFRP produced the greatest effect; however, the addition of GFRP for shear reinforcement also increased the stiffness of the beam nearly as much as the CFRP. If the CFRP wrapped part way up the sides were not present, the GFRP may have provided the larger effect. If the CFRP on the sides were not present, the stiffness increase due to the two composite systems may have been additive to give the stiffness of the S&F Beam. This effect was not investigated. However, it is believed that the stiffness increase was the result of the FRP reducing the width of cracks in the concrete.

It is important to realize that the Control Beam failed in shear before reaching its flexural capacity. Consequently, the capacity increases observed in the FRP-strengthened beams would not have been as significant if the Control Beam had been deficient in only flexure. However, the S&F Beam showed increased capacity compared to the S-Only Beam, a beam with adequate shear strength. This agrees with results from other researchers (GangaRao and Vijay 1998, Rostasy, et. al. 1992, Ritchie, et. al. 1991, Saadatmenesh and Ehsani 1991) that FRP is effective in strengthening flexurally deficient beams.

The deflection and strain at failure increased in the FRP-strengthened beams. Again, this occurred because the Control Beam had inadequate flexural and shear reinforcement initially. If

designed improperly, the addition of CFRP for flexure may increase the stiffness and decrease the deflection.

Table 4.1: Comparison of the strengthened beams to the Control Beam

Item	Control Beam Data	Percent Gain Over Control Beam[1]		
		F-Only	S-Only	S & F
Midspan Deflection at 15 kip (67 kN)	0.0465 in (1.18 mm)	3.2%	5.2%	-6.5%
Post Cracking Stiffness	115 kip/in (20.1 kN/mm)	21%	17%	30%
Maximum Observed Deflection	0.963 in (24.5 mm)	24 %	44 %[2]	3.8 %
Midspan Deflection at Failure	0.963 in (24.5 mm)	24 %	110 %[2]	No Failure
Load at Failure	107 kip (476 kN)	45 %	45 %	50 %[3]
Load at First Significant Cracking	17.6 kip (78.3 kN)	23 %	12 %	23 %
Maximum Applied Shear	53.5 kip (238 kN)	45 %	45 %	50 %
Maximum Applied Moment	321 kip-ft (435 kN-m)	45 %	45 %	50 %[4]

[1] 0% means equivalent to Control Beam results. Negative means lower than Control Beam results.
[2] Based on extrapolated deflection value.
[3] Based on the maximum applied load. Beam did not fail.
[4] Second load test of the S&F Beam reached a total applied moment of 640 kip-ft or 99% higher than the Control Beam.

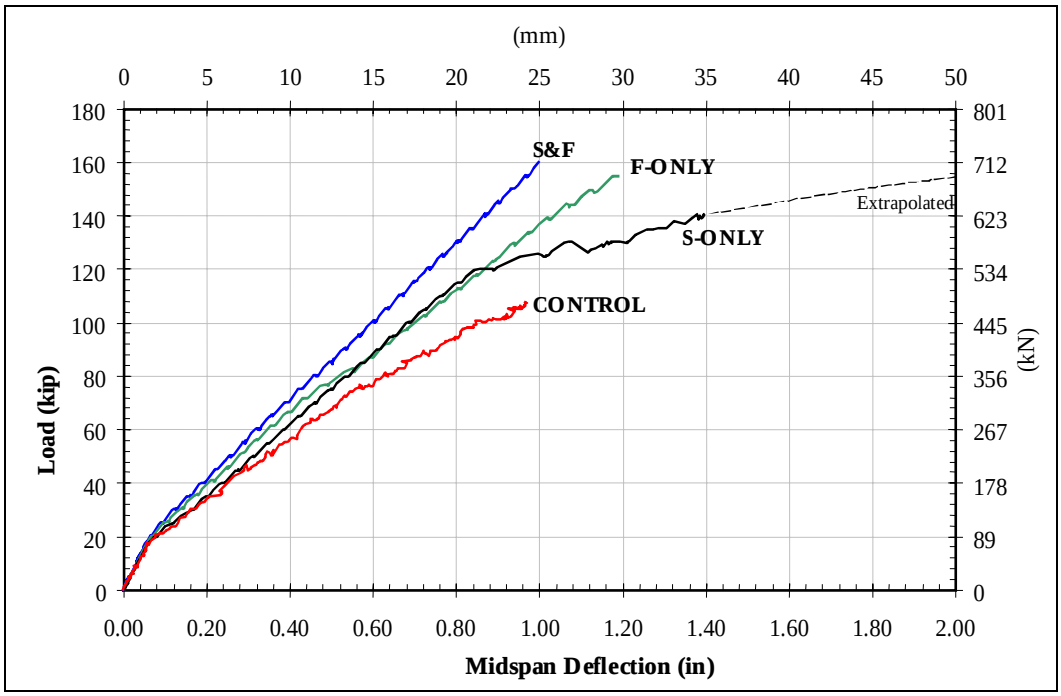

Figure 4.1: Load-deflection comparison of all experimental beams

4.2 MEETING THE TRUCK TRAFFIC LOADS

4.2.1 Moment Demand

Values from the load rating calculations performed by CH2M HILL and TAMS Consultants (CH2M HILL, 1997) are given in Table 4.2. These values are used in the following analysis for calculating the required capacity of the Horsetail Creek Bridge crossbeams.

The total factored load to be resisted by the applied live and dead loads is

$$\mathbf{M_u=\gamma_D M_{DL} + 1.3\gamma_L(1+I)M_{LL}} \qquad \mathbf{[4\text{-}1]}$$

where

γ_D=1.2,

γ_L=1.3 and

I= 0.10

such that: M_u=1.2*(82.3+25.0)+1.3*1.10*225, or M_u=451 kip-ft (611 kN-m)

To determine the required capacity of the fully reinforced element, the moment is divided by the strength reduction factor ϕ = 0.85 such that,

$$M_n=M_u/\phi=451/0.85$$

$$M_n=531 \text{ kip-ft } (720 \text{ kN-m})$$

Thus, the fully-reinforced, full-size beam should have supported at least a total applied moment of 531 kip-ft (720 kN-m). In third-point loading, this moment was not achievable with the given testing equipment. The maximum applied third-point moment was 480 kip-ft (651kN-m).

To confirm that the beam was adequate to reach this moment capacity and to potentially fail the beam, the S&F Beam was reloaded with the load points closer to the beam midspan. This loading produced a moment of 640 ft-kip (868 kN-m). According to the conservative design method adopted for the Bridge and shown in Appendix E, the S&F Beam moment capacity was 590 kip-ft (887 kN-m).

Table 4.2: Calculations from load rating (LRFD)

Item	Quantity
Moment @ midspan from bridge dead load	82.3 ft-kip (112 kN-m)
Moment @ midspan from wearing surface dead load	25.0 ft-kip (33.9 kN-m)
Maximum live load moment @ midspan from an HS20 truck	225 ft-kip (305 kN-m)
Shear @ critical section from bridge dead load	14.4 kip (64.1 kN)
Shear @ critical section from wearing surface dead load	4.50 kip (20.0 kN)
Live load shear @ critical section from HS20 truck	46.5 kip (207 kN)

4.2.2 Shear Demand

Similar calculations to those provided in the above discussion show the total factored shear force to be,

$$V_u=\gamma_D V_{DL} + 1.3\gamma_L(1+I)V_{LL} \qquad [4\text{-}2]$$

where

γ_D=1.2,

γ_L=1.3 and

I= 0.10

such that: V_u=1.2*(14.4+4.50)+1.3*1.10*46.5, or V_u=83.1 kip (370 kN)

To determine the required capacity of the Horsetail Creek Bridge crossbeam, the required strength is divided by the reduction factor ϕ = 0.85 such that,

$$V_n=V_u/\phi=83.1/0.85$$

$$V_n=97.8 \text{ kip } (435 \text{ kN})$$

The maximum shear force near the supports achieved during testing was ½ of 160 kip or 80 kip (356 kN). The actual capacity of the beam was not verified in shear, although conservative calculations based on the design method outlined in Appendix E showed the capacity to be 107 kip (476 kN).

The required, pre-strengthened, and post-strengthened bridge capacities based on calculations are shown in Table 4.3. Testing of the S&F Beam verified that the strengthened Horsetail Creek Bridge beams have at least the required moment capacity. Since the S&F Beam test had to be stopped before reaching the required shear load level of 98 kip (436kN), the moment capacity of the Horsetail Creek Bridge beams was not verified. However, conservative design calculations indicate the shear capacity of the Horsetail Creek Bridge beams should be 107 kip (476 kN). It should be noted that the small differences in S&F Beam design values given above and the Horsetail Creek Bridge design values shown in the table are due to the difference in concrete properties (Table E-2) used in the calculations.

Table 4.3: Capacities of the full-size beams and the Horsetail Creek Bridge crossbeams. The values shown for the full-size beams are measured values. The values for Horsetail Creek Bridge are calculated values.

	Control	**F-Only**	**S-Only**	**S&F[1]**	**Horsetail Creek Bridge**		
					Required[2]	**Before Strengthening[3]**	**After Strengthening[4]**
Failure Mode	Shear	Shear	Flexure	Expect flexure	Flexure	Expect shear	Expect flexure
Shear Capacity, kip (kN)	54 (240)	78 (347)	N/A	>80 (356)	98 (436)	34 (151)	107 (476)
Moment Capacity, kip-ft (kN-m)	N/A	N/A	465 (630)	>640 (868)	531 (720)	341 (462)	569 (771)

[1]Beam did not fail. Values shown are based on maximum levels applied during the test.
[2]Based on Load and Resistance Factor Method.
[3]Based on Ultimate Strength Design method.
[4]Based on design method outlined in Appendix E.

5.0 CONCLUSIONS AND RECOMMENDATIONS

5.1 CONCLUSIONS

- The unstrengthened Horsetail Creek Bridge crossbeams would have failed in shear at approximately 53 kip (236 kN) shearing force. The beams were substantially deficient in shear based on conventional calculations that showed the dead and live load shear acting on the bridge was 65.4 kip (291 kN).

- The strengthened Horsetail Creek Bridge crossbeams, which are retrofitted with both the GFRP for shear and CFRP for flexure, have at least 50% more static load shear capacity over the unstrengthened beams. The test had to be stopped at an applied shear of 80 kip (356kN) due to equipment limitations before reaching the 98 kip (436 kN) level required by traffic loads.

- The strengthened Horsetail Creek Bridge crossbeams have at least 99% more static load moment capacity than the unstrengthened beams. The fully reinforced beam exceeded the demand of 531 kip-ft (720 kN-m) by sustaining up to 640 kip-ft (868 kN-m) applied moment.

- The strengthened Horsetail Creek Bridge crossbeams are 30% stiffer than the unstrengthened beams.

- Horsetail Creek Bridge crossbeams retrofitted with only the flexural CFRP would still result in diagonal tension failure albeit at a more substantial load of 155 kip (689 kN). The CFRP was wrapped up the sides a sufficient amount to provide resistance across the diagonal tension crack. In addition, the increased stiffness provided by the CFRP decreased the deformation and offset cracking by reducing strain in the beam. However, this load increase should not be relied upon in design.

- Horsetail Creek Bridge crossbeams retrofitted only with the GFRP for shear would fail in flexure at the midspan at 155 kip (689 kN). Yielding of the main flexural steel would initiate prior to crushing of the concrete

- The addition of GFRP for shear was sufficient to offset the lack of stirrups and cause conventional RC beam failure by steel yielding at the midspan. This allowed ultimate deflections to be 200% higher than the shear deficient Control Beam, which failed due to a diagonal tension crack.

- Load at first significant crack was increased, primarily due to the added stiffness of the flexural CFRP, by approximately 23%. The added stiffness reduced the deflections, which in turn reduced the strains and stresses in the cross section for a given load.

5.2 RECOMMENDATIONS

The S&F Beam should be loaded to failure to determine the capacity and verify the failure mode of the strengthened Horsetail Creek Bridge crossbeams.

6.0 REFERENCES

AASHTO Subcommittee on Bridge and Structures. 1989. *Guide Specifications for Strength Evaluation of Existing Steel and Concrete Bridges*. American Association of State and Highway Transportation Officials.

AASHTO Subcommittee on Bridge and Structures. 1994. *Manual for Condition Evaluation of Bridge*. American Association of State and Highway Transportation Officials.

ACI. 1995. *Building Code Requirements for Structural Concrete: ACI 318-95*. American Concrete Institute, Committee 318.

American Society for Testing and Materials (ASTM) Subcommittee C09.70. 1994. *Standard Test Method for Static Modulus of Elasticity and Poisson's Ratio of Concrete in Compression*. Designation C 469-94, ASTM, Philadelphia.

American Society for Testing and Materials (ASTM) Subcommittee C09.64. 1983. *Standard Test Method for Pulse Velocity Through Concrete*. Designation C 597-83, ASTM, Philadelphia.

CH2M HILL, Inc., Consulting Engineers, Corvallis, Oregon – in conjunction with TAMS Consultants. 1997. "Evaluation and Resolution of Under Capacity State Bridges: Bridge #04543, Horsetail Creek Bridge." June.

Cooper, J.D. 1990. "A New Era in Bridge Engineering Research." *2nd Workshop on Bridge Engineering Research in Progress*. NSF, Reno, Nevada, pp. 5-10.

FHWA. 1993. "National Bridge Inventory in Highway Bridges Replacement and Rehabilitation Program: 11th report of the Secretary of Transportation to the United States Congress." Washington, D.C.

FHWA. 2000. J.M. Hooks, "Advanced Composite Materials for the 21st Century Bridges: The Federal Highway Administration Perspective," published in *Innovative Systems for Seismic Repair & Rehabilitation of Structures*. Technomic Publishing Co, Inc., Pennsylvania.

GangaRao, H.V.S., P.V. Vijay. 1998. "Bending Behavior of Concrete Beams Wrapped with Carbon Fabric." *Journal of Structural Engineering*, ASCE, Vol. 124, No. 1, Jan., pp. 3-10.

Kachlakev, Damian. 1998. *Strengthening of the Horsetail Creek Bridge Using Composite GFRP and CFRP Laminates.* Prepared for the Oregon Department of Transportation, March 1998.

Ritchie, P.A., et. al. 1991. "External Reinforcement of Concrete Beams Using Fiber Reinforced Plastics." *Structural Journal*, ACI, Vol. 88, No. 4, pp. 490-496.

Rizkalla, S., P. Labossiere. 1999. “Planning for a New Generation of Infrastructure: Structural Engineering with FRP – in Canada.” *Concrete International*, Oct., pp. 25-28.

Rostasy, F.S., C. Hankers, E.H. Ranisch. 1992. “Strengthening of R/C- and P/C-Structures with Bonded FRP Plates.” *Advanced Composite Materials in Bridges and Structures*. ACMBS-MCAPC, K.W. Neale and P. Labossiere, Editors. Canadian Society for Civil Engineering, pp. 255-263.

Saadatmanesh, H., M.R. Ehsani. 1991. “RC Beams Strengthened with GFRP Plates I: Experimental Study.” *Journal of Structural Engineering*, ASCE, Vol. 117, No. 11, Nov., pp. 3417-3433.